IEEE Access
Multidisciplinary | Rapid Review | Open Access Journal

Received October 23, 2021, accepted November 13, 2021, date of publication November 16, 2021,
date of current version November 24, 2021.

Digital Object Identifier 10.1109/ACCESS.2021.3128467

Identification of Lap Joint Dynamics Using Interfacial Nanocomposite Force Sensor

MEHDI SANATI, HAMID MOSTAGHIMI, ALLEN SANDWELL, JIHYUN LEE, AND SIMON S. PARK

Department of Mechanical and Manufacturing Engineering, University of Calgary, Calgary, AB T2N 1N4, Canada

Corresponding author: Simon S. Park (simon.park@ucalgary.ca)

This work was supported by the Natural Sciences and Engineering Research Council of Canada (NSERC) under the Canadian Network for Research and Innovation in Machining Technology (CANRIMT) Strategic Research Network Grant NETGP 479639-15.

ABSTRACT Machine tools are complex structures consisting of several parts connected through different types of joints. Mechanical joints affect dynamics of the machine tools significantly, and any virtual model of the structure should include joint properties. It is desirable to use an interfacial sensor inside the joint to directly identify joint dynamic properties without changing the joint's design and dynamics. In this study, a polymeric nanocomposite sensor with high sensitivity and a wide frequency bandwidth is implemented inside a bolted lap joint to identify the joint dynamic properties. The sensor implementation does not require any modifications to the joint design which makes the proposed approach suitable for many applications. An identification procedure is developed to find the micro-slip regime and the stick-slip boundaries in the joint interface using the acquired data of the nanocomposite sensor. Lab scale experiments are then conducted on a structure that consists of two beams attached to each other using a bolted lap joint. The proposed method is then used to identify the joint dynamics and the results are then compared with an existing approach named hysteresis loop technique. The experimental results show that the proposed method can predict the joint properties effectively with maximum deviations of 17% compared to the hysteresis loop results. Furthermore, effects of the contact normal load and the excitation load on the joint properties are investigated.

INDEX TERMS Bolted lap joint, joint dynamics, nanocomposite sensor, hysteresis loop, experiment.

I. INTRODUCTION

The fourth industrial revolution aims to employ the modern technology to automate the conventional manufacturing and industrial processes through real-time sensing and monitoring of complex systems. This improves the efficiency and quality of the finished products and reduces manufacturing wastes. Therefore, with the advent of Industry 4.0 and the digital transformation of manufacturing processes, the accurate design, identification, and condition monitoring of machine tools are becoming critically important. Machine tools consist of many components including plates, bars, beams, etc. assembled through different types of joints such as bolts, screws, bearings and guideways. To develop an accurate virtual model of the machine tools, the dynamic properties of all the components of the structure should be identified. Dynamic properties of the machine tools highly depend on the mechanical joints that exist within the assembly.

Bolted lap joints are one of the most common type of joint connections used in assembled structures. They have a wide range of applications in automotive industries, machine tools, and civil structures such as bridges. Bolted joints are one of the main sources of energy dissipation in assembled structures due to the slip mechanism of the contact area [1]. These types of joints cause discontinuity in the structure and can result in high stress concentrations in the contact areas.

Different analytical and numerical methods have been proposed to model the joint mechanics and to identify the joint properties. The early models introduced by Iwan [2] used parallel and series combinations of elastoplastic elements to model hysteresis effects of the joints. These models included both micro-slip and macro-slip movements within the contact area of the joint. Later, it was shown that the models with elastoplastic elements arranged in series provide a more realistic representation of the deformations that occur in the

The associate editor coordinating the review of this manuscript and approving it for publication was Jingang Jiang.

This work is licensed under a Creative Commons Attribution 4.0 License. For more information, see https://creativecommons.org/licenses/by/4.0/

vicinity of the contact area [3]. An adjusted model based on Iwan's beam model was developed to analyze the dynamic response of the two beams attached through mechanical joints [4].

Mechanical joints are also subjected to the nonlinearities of their stiffness and damping properties, in particular, adjacent to the connection points where a higher contact stress exist. Many decoupled and coupled methods have been developed over the past years to represent the joint properties [5]. To address the computational cost and dependency of the Iwan's model to the excitation range, a new distribution of the dry friction was proposed by introducing a new transition regime from the micro-slip to macro-slip [6]. Although computationally efficient, the joint identifications process of the decoupled and coupled models are not straightforward and are limited to low amplitude excitations [5]. This led to the development of more comprehensive discretized models that address the nonlinearities involved [7], and to novel optimization algorithms [8] that facilitate the joint dynamics identification process.

Numerical simulation of the joints can also be done for structures with more complexity. The finite element (FE) models are usually constructed based on node-to-node contact, thin layer elements, and zero thickness elements [9]. These models have been widely used to identify the nonlinear stiffness and damping of the bolted lap joints [10], and to predict the contact stress of a bolted joint by implementing a pressure-sensitive film inside the joint [11]. The main challenges associated with the application of FE methods to identify joint dynamics are the difficulties related to defining the surface roughness, contact behaviors, constraints, and significant computational time. Additionally, an accurate estimation of the modal parameters is usually required, particularly for highly damped systems and systems with closely coupled modes [12]. This makes the models highly sensitive to the contact and modal parameters.

The experimental approach can also be used to identify joint dynamics and the contact pressure distribution. Sanati *et al.* [13] developed an experimental approach to identify damping of the bolted joints subjected to both translational and rotational vibrations. Furthermore, the inverse receptance coupling method that combines experimental and simulation results has been shown to be an effective method to predict the joint dynamics in 3D structures [14] and in the lap joints [15]. Several studies have proposed the idea of instrumenting a joint [16] to measure the contact forces. However, an instrumented bolt requires some modifications on the joint assembly to retrofit a load-cells or a series of strain gauges, which alters dynamics of the system, considerably.

This study aims to introduce an experimental approach to identify dynamic properties of a bolted lap joint under a wide range of loading conditions. The proposed experimental method does not suffer from the limitations associated with the analytical and numerical methods. The main novelty of this study is to measure the joint dynamic properties directly by implementing a thin nanocomposite sensor inside the joint. The nanocomposite sensor that exhibits both piezoresistive and piezoelectric characteristics, is sandwiched between a bolted lap joint with minimum effects on the joint design and on the dynamics of the system. The nanocomposite sensor along with the proposed identification technique are then employed to study the micro-slip regime in the joint interface and eventually, to extract the joint dynamic properties. The micro-slip regime is the dominant phenomenon in the bolted lap joints when a proper tightening torque is applied to the bolts. The proposed experimental approach is finally tested to investigate effects of different parameters, including normal load and excitation load, on the dynamic properties of the joint. Once the feasibility is proven, the proposed methodology can be utilized for other applications such as online measurements and monitoring of structures and processes.

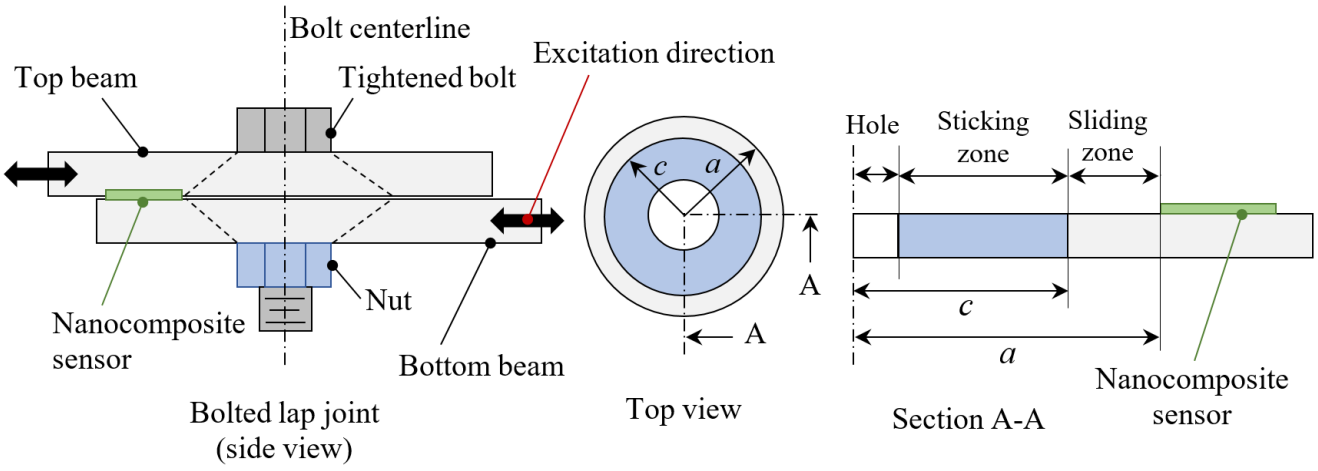

FIGURE 1. The schematic of the assembled joint structure (left) and different boundaries at the joint interface (right).

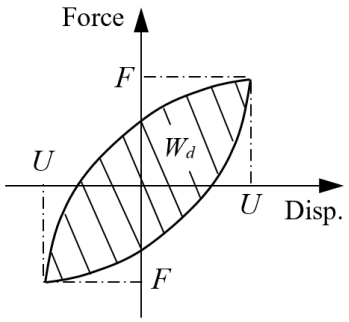

FIGURE 2. The schematic of a typical hysteresis loop.

II. CONTACT JOINT MODELS

When an external force is applied to a pre-tightened bolted joint perpendicular to the bolt's centerline, slipping occurs at certain regions of the joint contact zone and this localized motion is usually referred as the micro-slip motion. As the applied force increases, the micro-slip region becomes larger, and once it reaches a certain level, the entire contact area starts to slip. This is known as macro-slip behavior of the joint, which allows the relative motion between the components due to the excitation force. When the excitation level remains below the macro-slip threshold, only the micro-slip motion is present in the contact zone of the joint; however, due to the non-uniform pressure distribution within the joint, the contact area can be divided into sticking and sliding zones. The stick-slip boundary should be determined to be used for development of the joint contact model. The model is then used to predict stick-slip behavior of the lap joint and to extract the friction force, energy loss, and the joint properties.

The joint interface in the micro-slip level of the motion can be divided into two different regions, including the contact zone and the non-contact zone [17]. Micro-slip motion within the contact zone starts from the outer regions due to the lower pressure on those areas. Therefore, the inner and the outer areas of the contact zone are called sticking and sliding zones, respectively. Fig. 1 shows a joint consisting of two substructures (beams) connected through a pre-tightened bolt. Each of the beams is excited longitudinally, i.e., perpendicular to the bolt's centerline. During each loading cycle, the width of the slip annulus (a-c) grows from zero to maximum, corresponding to the maximum displacement applied to the structure, and then shrinks back to zero [18] as the excitation on the system is removed. The radius a illustrates the boundary between the contact zone and non-contact zone; the radius c shows the boundary between the sticking zone and the sliding zone. To minimize the impacts of the nanocomposite sensor on the joint interface, the sensor is installed away from the bolted area.

A. JOINT IDENTIFICATION THROUGH HYSTERESIS LOOP

Joint dynamics can be identified using hysteresis loop method based on the force-displacement curve. The shear force is measured by the nanocomposite sensor implemented inside the joint, and the relative displacement of the bolted beams is measured by using external sensors. Fig. 2 shows a typical hysteresis loop with the energy loss of W_d, and the maximum displacement of U when the maximum force of F is applied. The energy loss in the system can be obtained by computing the enclosed area. For a structure containing a bolted lap joint, the energy loss can be mostly attributed to the energy dissipated through friction in the joint interface.

$$C = W_d/\left(\pi\omega U^2\right) \tag{1}$$

The damping of the joint C can be found using the energy loss, excitation frequency ω, and displacement amplitude of the structure under harmonic excitation. The slope of the hysteresis loop also shows the stiffness of the joint [19].

B. JOINT IDENTIFICATION USING STICK-SLIP BOUNDARY

The dynamic properties of the bolted lap joints can be identified once the frictional force and the total energy loss within the joint have been determined. However, the process requires knowledge of the stick-slip boundary at the joint interface. The boundary between the contact zone and the non-contact zone can be determined using the contact stress distribution within the joint interface. This boundary is defined as the radius where the contact stress is zero. According to Fig. 3, the stress distribution within the contact interface of the layered bolted structures can be defined in a non-dimensional form as below [20]:

$$\frac{\sigma}{\sigma_s} = \sum_{n=0}^{5} A_n \left(\frac{r}{r_b}\right)^{2n} \tag{2}$$

where A_n are constant coefficients provided in Table 1, σ_s is the applied stress under the bolt head and σ is the

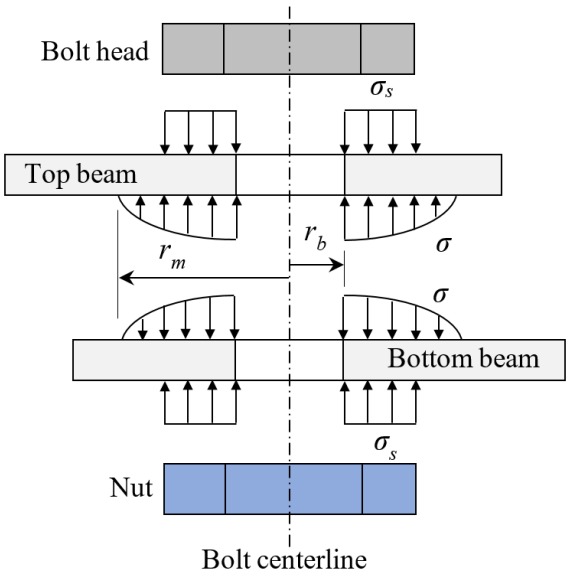

FIGURE 3. The free-body diagram of a lap joint illustrating the contact zone [20].

non-uniform pressure distribution between the top and bottom beams. The uniform stress applied from the bolt to the beams can be found by measuring the normal force applied to the structure and the area under the bolt head. According to (2), the border between the contact zone and the non-contact zone is independent of the tightening load applied to the joint. A circular border with 3.5 times the bolt radius can be considered as the non-contact boundary of the joint, i.e., $a = 3.5r_b$ [20].

The only remaining unknown is the boundary between the sticking and sliding zones. This boundary can be found since frictional forces in the sticking and the sliding zones are equal at the boundary. The frictional force in the sliding zone f_{sld}, is obtained as a function of the contact stress and friction coefficient as follows,

$$f_{sld} = 2\pi \int_c^a \mu\sigma r dr \tag{3}$$

where μ is the friction coefficient measured experimentally, σ is the contact stress distribution given in (2), a is the boundary radius between the contact and non-contact zones, c is the boundary radius between the sticking and sliding zones, and r is the radius. To find the frictional force in the sticking zone, an elastic shear layer with negligible thickness is considered in the joint interface [21]. This elastic layer acts as a shear spring connected to the beams in the sticking zone, and allows every contact point to have an elastic displacement relative to the support before slipping [22]. This linear deformation of the contact points in the sticking zone occurs due to asperities or bonding contact stress. Thus, the frictional force in the sticking zone f_{stk}, is considered as below:

$$f_{stk} = K_t u \quad |K_t u| \leq f_{\max} \tag{4}$$

where K_t is the stiffness of the shear layer in the tangential direction and can be identified experimentally. The yield level or the sliding threshold is f_{max}, and u represents the relative displacement of the bolted beams along the axial direction. The efficient joint identification algorithm based on (3) and (4) is then developed to find the stick-slip boundary of the bolted lap joint.

In this algorithm, the assembled structure presented in Fig. 1 needs to be excited harmonically at the frequency of ω in the axial direction. The amount of energy dissipated due to the frictional forces in one vibration cycle is four times of the energy dissipated in a quarter of a cycle [18]; thus, the amount of energy dissipated in the first quarter of a cycle is calculated and multiplied by four to find the energy loss in a full cycle. This will reduce the computational time. The following steps are designed to identify the stick-slip boundary and the dynamic properties of the joint. First, n samples of the relative displacement of the beams, corresponding to the first quarter of the cycle, are selected as below.

$$\begin{cases} u_i & i = 1, 2, \ldots, n \\ u_1 = 0 \end{cases} \tag{5}$$

where u_i is the i^{th} relative displacement. Then, for each specific u_i, the stick-slip boundary c_i, is determined by equating the frictional force of the sliding and sticking zones.

$$\int_{c_i}^a \mu\sigma(2\pi r)dr = K_t u_i \tag{6}$$

where σ is the contact stress distribution and K_t is the stiffness of the elastic shear layer. The latter is assumed to be constant throughout the identification process under certain level of excitation and loading conditions.

The obtained stick-slip boundary is then used to calculate the frictional force and the energy loss inside the joint interface. Next, the energy loss is calculated using the boundary obtained through micro-slip analysis. The total amount of energy loss in each step is:

$$W_{di} = 4\left(2\pi\mu\Delta u_i \int_{c_i}^a \sigma r dr\right) \tag{7}$$

where $\Delta u_i = u_i - u_{i-1}$. Having the energy loss of each step of the calculations, the equivalent damping coefficient and stiffness of the joint are obtained as below:

$$C_i = \frac{\sum_{i=2}^{n} W_{di}}{\pi\omega u_i^2} = \frac{8\pi\mu \sum_{i=2}^{n}\left(\Delta u_i \int_{c_i}^a \sigma r dr\right)}{\pi\omega u_i^2} \tag{8}$$

$$K_i = \frac{F_i}{u_i} = \frac{f_{stk} + f_{sld}}{u_i} = \frac{2K_t u_i}{u_i} = 2K_t \tag{9}$$

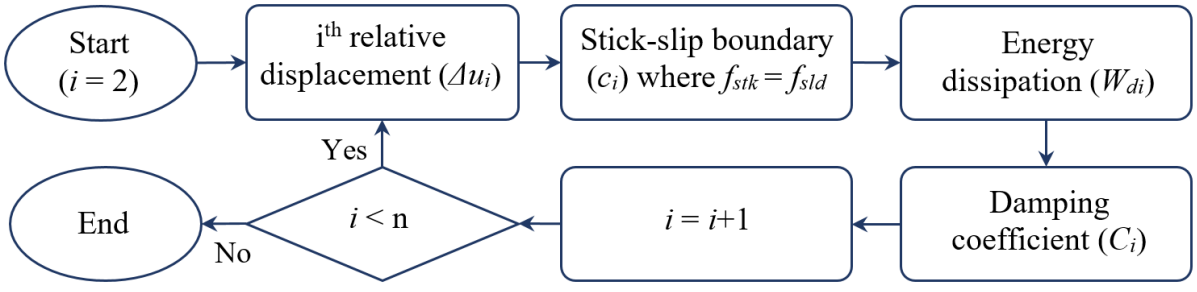

FIGURE 4. The flowchart of the joint identification algorithm to identify damping coefficient.

TABLE 1. The constants coefficients of the polynomial used for pressure distribution of the contact interface [20].

Constant	Value	Constant	Value
A_0	0.68517	A_3	0.23895×10^{-2}
A_1	0.10122	A_4	0.29487×10^{-3}
A_2	0.94205×10^{-2}	A_5	0.11262×10^{-4}

where C_i, K_i and F_i are respectively the ith joint damping coefficient, joint stiffness, and the contact force. The process is then continued for each of the n samples.

Fig. 4 shows the flowchart of the proposed joint identification algorithm that provides the real-time stick-slip boundary of the joint and variation of the damping coefficient while the joint is excited. It is worth mentioning that the friction coefficient μ, and the stiffness of the elastic shear layer K_t, are identified experimentally prior to using in the proposed algorithm. These identified values will be presented in the results section.

III. EXPERIMENTAL SETUP

The proposed experimental approach requires a setup to excite a bolted joint harmonically with different frequencies and amplitudes to measure the contact forces and relative displacements of the joint components. Therefore, a customized experimental setup is developed and a testing procedure is defined to identify the joint dynamic properties. A polymer-based nanocomposite sensor is prepared and then is implemented inside the bolted lap joint to measure the tangential contact force. To minimize the effects of the nanocomposite sensor on the joint properties, the sensor is installed away from the bolted area. However, the sensor remains in contact with the bolted beams due to its thickness. This method of sensor implementation reduces the undesirable effects of sensor on the stick-slip boundaries. The measured forces and relative displacement of the joint components are then used to identify the hysteresis loop and the stick-slip boundary at the joint interface and finally to verify the feasibility of the proposed experimental approach.

A. NANOCOMPOSITE SENSOR

A highly sensitive, very thin, polymer-based nanocomposite sensor is developed [23] that provides the piezoelectric and piezoresistive properties in a single sensor. Therefore, it covers a wide frequency bandwidth compared to many commercial sensors, which are suitable for either low or high frequency measurements. This cost-effective sensor can be sprayed even on non-flat surfaces within the joint, which broadens its applications. The developed nanocomposite sensor can measure the tangential forces directly after calibration without any extra calculations. According to Fig. 5, polyvinylidene fluoride (PVDF) is used as the polymer matrix to develop the nanocomposite sensor. The PVDF polymer provides piezoelectric properties for the sensor, which is used for high frequency measurements. Adding carbon nanotubes (CNT) to the polymer matrix improves the conductivity of the nanocomposite sample and provides piezoresistive properties, which can be used for low frequency measurements. The CNT concentrations have been chosen close to the percolation threshold to optimize the piezoelectric and piezoresistive performance of the sensor. The fabrication process includes several steps. First, a solution of PVDF (100 nm powder) and dimethylformamide (DMF) with the ratio of 0.1 g/mL is prepared. The solution is then stirred on a hot plate at 80 °C for 3 hours. Next, CNT particles with a concentration of 0.0004 g/mL are separately mixed in DMF and the solution is sonicated at room temperature for 30 minutes to achieve a homogeneous dispersion of nanoparticles. The prepared solutions are then mixed and stirred for one extra hour at the room temperature. A thin layer of the PVDF-CNT mixture with the thickness of 70 μm is then deposited on a solid substrate using spray coating method and is heated at 80 °C until the solvent (DMF) is fully evaporated.

The piezoelectric properties of the sensor are further improved by applying two sequential processes of mechanical stretching and high-voltage electrical poling. These processes activate the piezoelectric properties of the PVDF polymer and improve the sensitivity of the sensor. The prepared samples are stretched mechanically at the temperature of 80 °C, which results in up to 500 percent elongation on the samples. This process improves the β-phase of the sensor, which is associated with the piezoelectricity of PVDF. Although the stretching process increases the β-phase of the sample, the dipoles are still randomly arranged. The exposure of the stretched sample to a high electric field provides the alignment of the dipoles and results in a high piezoelectric coefficient, i.e., d_{33}. A corona poling setup [23], consisting of a high-voltage power supply (15 kV), a metallic grid mesh, a voltage divider, a corona needle and a copper electrode are used to apply a high voltage electric field to the sensor. Once the fabrication process of the nanocomposite sensor is completed, the sensor is covered by copper electrodes and is laminated with thin plastic layers. Finally, the sensor is implemented inside the joint interface to measure the tangential force.

B. JOINT EXCITATION SETUP

The joint excitation setup consists of two beams attached together using a mating bolt and nut (see Fig. 6). The beams are connected to two shakers (Bruel & Kjaer 4808) through mechanical links and are excited in axial direction simultaneously. A force sensor (Kistler 9018B) is used to measure the input forces from the shakers and two capacitive sensors (Lion DMT20) with the sensitivity of 80 V/mm, are used to measure the relative displacement of the bolted beams. The interfacial nanocomposite sensor also measures the contact shear forces during harmonic excitation of the beams.

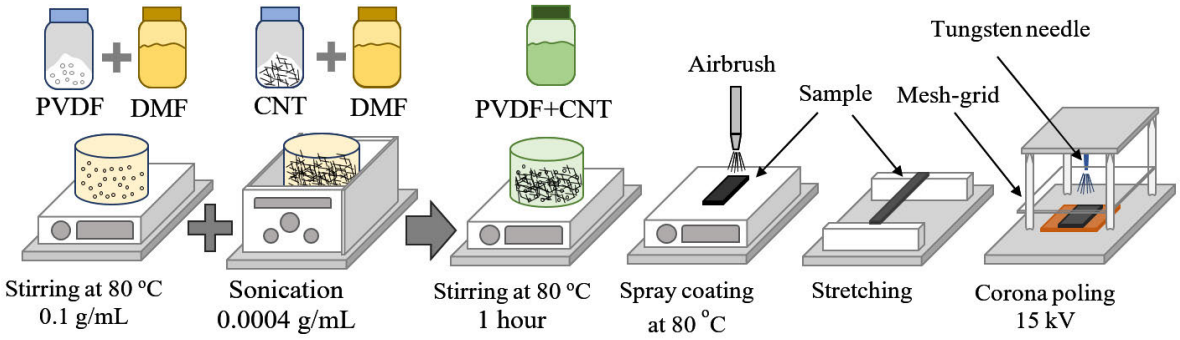

FIGURE 5. The schematic of the nanocomposite sensor fabrication process.

The shakers are fed using a single function generator (Tektronix AFG1022) and two power amplifiers (Bruel & Kjaer 2712A) to excite the beams with the same inputs (frequency and amplitude) but in the opposite directions. To ensure the same excitation load from both sides, each shaker is separately tested using the force sensor and the gain is adjusted accordingly prior to performing the experiments. The measurements of all the sensors are amplified and recorded through proper data acquisition systems (NI 9233 DAQ).

The joint properties are first identified by applying 5 Nm of tightening torque to the bolt and exciting the joint with the frequency of 400 Hz and amplitude of 20 V peak to peak (PP). This results in a calibration factor of 301 N/V for

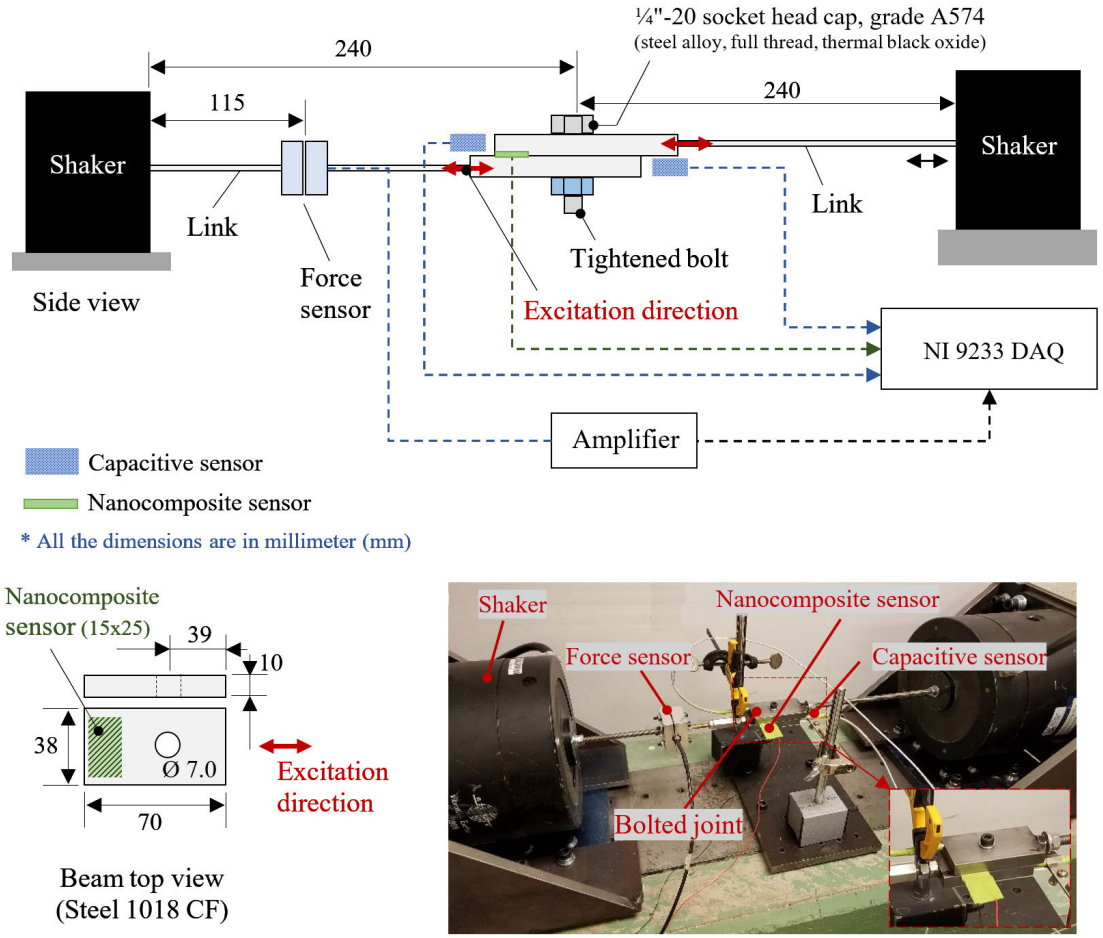

FIGURE 6. The schematic of the experimental setup (top) and the manufactured setup (bottom) for the identification of the joint dynamic properties.

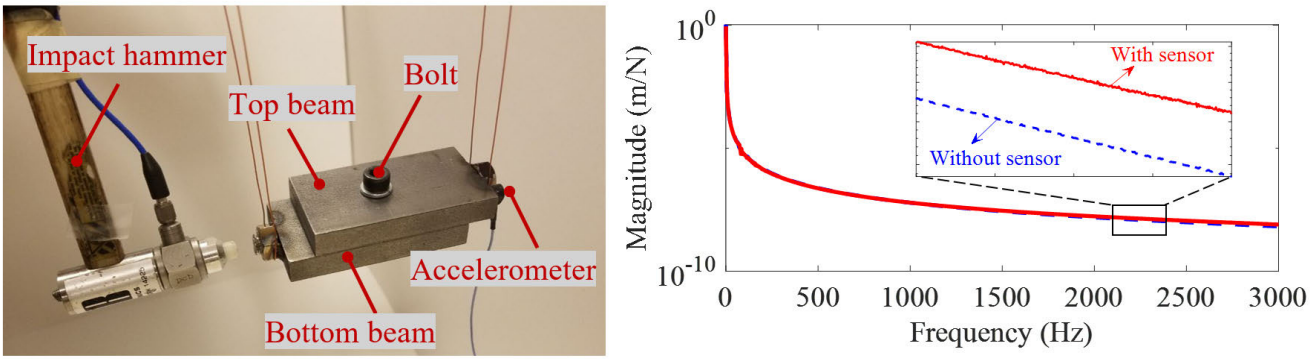

FIGURE 7. The experimental setup used for extracting FRF (left) and comparison of the joint FRF with and without nanocomposite sensor (right).

the nanocomposite sensor. This calibration factor is almost constant for a certain range of frequencies at all the excitation amplitudes investigated; however, it varies for other frequency ranges. This is most likely caused by the compression of the nanocomposite sensor between the two beams that occurs while measuring shear forces. The tightening torque and amplitude of the excitation will then be varied when sensitivity analysis of the influential parameters is conducted. Implementing a nanocomposite sensor inside the bolted structure may change the dynamics of the structure slightly. Thus, an experimental modal analysis is performed on the bolted joint with and without the nanocomposite sensor to investigate if the implementation of our sensor alters the system dynamics. Fig. 7 shows the bolted structure with free-free boundary condition excited by an impulse hammer (PCB 2222); the acceleration of the structure is measured using an accelerometer (Kistler 8778A500). Comparison of the magnitude of the FRF shows that the dynamics of the bolted structure does not change when the nanocomposite sensor is implemented inside the joint. Therefore, it is assumed that the joint properties are not affected by the nanocomposite sensor.

IV. RESULTS AND DISCUSSION

The hysteresis loop method, along with the proposed joint identification algorithm, are used to identify the dynamic properties of the bolted lap joint. The effects of two influential parameters, namely the excitation load and the contact normal load on the bolt, are then investigated. The joint identification algorithm has some advantages compared to the hysteresis loop method. The joint identification algorithm provides detailed information about the joint interface such as the stick-slip boundaries, and nonlinear values of the joint damping as a function of the relative displacement of the beams, which are not achievable using the hysteresis loop method. Additionally, there are many applications where installation of force sensors externally is not possible while a thin-layered nanocomposite sensor can be readily implemented.

A. IDENTIFIED JOINT PROPERTIES

The friction coefficient in the joint interface can be obtained while the joint experiences macro-slip movements. The friction coefficient is a property of the joint interface and independent of the type of motion. The experimental setup shown in Fig. 6 is used for this purpose. High frequency excitations and high tightening torque results in micro-slip motion at the joint and cannot be used for identification of the friction coefficient. Therefore, the joint is excited at a lower frequency of 100 Hz with the tightening torque of 2 Nm to extract the friction coefficient. The measurements of the nanocomposite sensor is then converted to the frictional force through the calibration factor found in the previous section. With knowledge

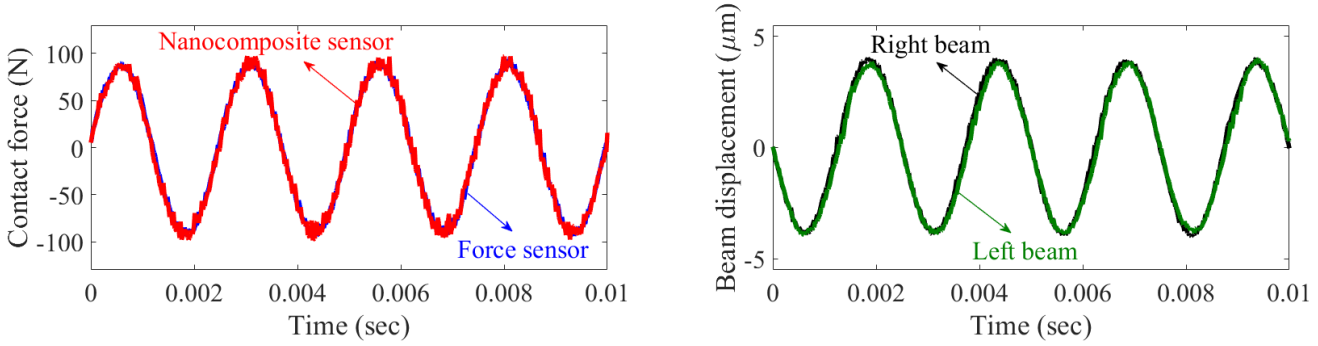

FIGURE 8. The measured contact forces using the reference force sensor and the nanocomposite sensor (left), and the measured beam displacements using the capacitive sensors (right) under the reference loading condition.

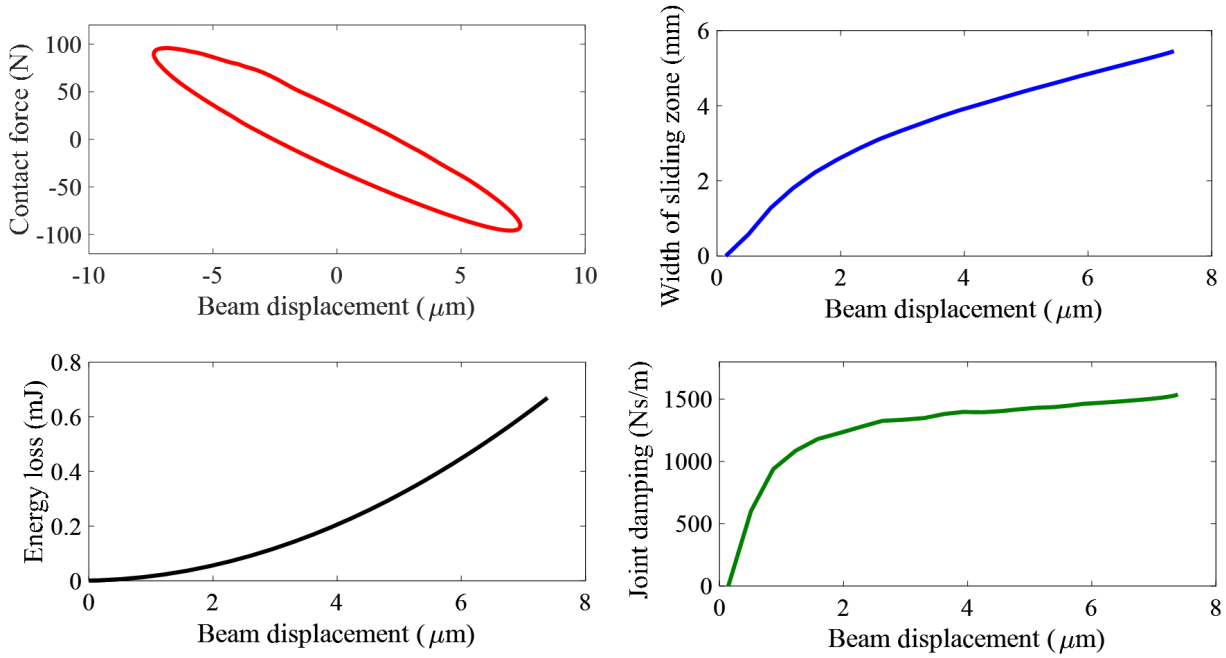

FIGURE 9. The hysteresis loop (top-left), the identified stick-slip boundary (top-right), the energy loss (bottom-left), and the joint damping (bottom-right) extracted under the reference loading condition.

of the normal force due to the tightening torque, and the friction force measured by the nanocomposite sensor, the friction coefficient is obtained as:

$$\mu = \frac{f_{sld}}{f_n} = \frac{161.1}{956.3} = 0.168 \tag{10}$$

where f_{sld} and f_n are friction force and normal force, respectively. The ratio between the tightening torque and the normal force applied to the joint was experimentally determined to be 478.0 N/Nm using the force sensor.

Fig. 8 shows the measured contact forces using the reference force sensor and the nanocomposite sensor, and the measured beam displacements using the capacitive sensors at the excitation frequency of 400 Hz, tightening torque of 5 Nm and the excitation amplitude of 20 V-PP, as the reference loading condition. The measured data are then filtered using a zero-phase 5th order Butterworth lowpass filter with a cut-off frequency of 3000 Hz.

Fig. 9 shows the stick-slip boundary (top-right), the energy loss (bottom-left), and the joint damping (bottom-right) under the reference loading condition, identified from the proposed joint identification algorithm. Fig. 9 (top-left) also shows the hysteresis loop of the joint, which clearly exhibits a micro-slip regime inside the joint interface. The area inside the hysteresis loop is computed to obtain the energy loss and the joint damping is then identified based on the energy loss, excitation frequency and maximum relative displacement. Additionally, the joint stiffness is calculated from the slope of the hysteresis loop. The energy loss, joint damping and joint stiffness are found to be 0.809 mJ, 1867 Ns/m, and 11.8 MN/m based on the hysteresis loop. According to the results of the joint identification algorithm, the maximum energy loss and joint damping coefficient are obtained as 0.672 mJ and 1542 Ns/m. In addition, the damping coefficient changes while the joint is excited. This is due to the change in the stick-slip boundary of the joint, which cannot be obtained from the hysteresis loop. Furthermore, results show that there is no joint damping at the beginning of the excitation since there is no sliding and minimal energy loss. Table 2 compares the joint properties identified using the joint identification algorithm and the hysteresis loop. There is approximately 17 percent deviation between the energy loss and the damping coefficient obtained from the proposed methods. The deviation is mostly due to the nonlinearity in the joint interface and the simplifications associated with the stick-slip boundary of the joint.

TABLE 2. The joint properties identified using the joint identification algorithm and the hysteresis loop.

Joint property	Unit	Method		
		Joint Identification algorithm	Hysteresis loop	Diff. (%)
Energy loss	mJ	0.672	0.809	17.1
Joint damping	Ns/m	1542	1867	17.4
Joint stiffness	MN/m	-	11.8	-

Despite the small deviation between the joint properties obtained from the joint identification algorithm and the hysteresis loop, the proposed sensor-based method can be used to measure the contact forces and the joint

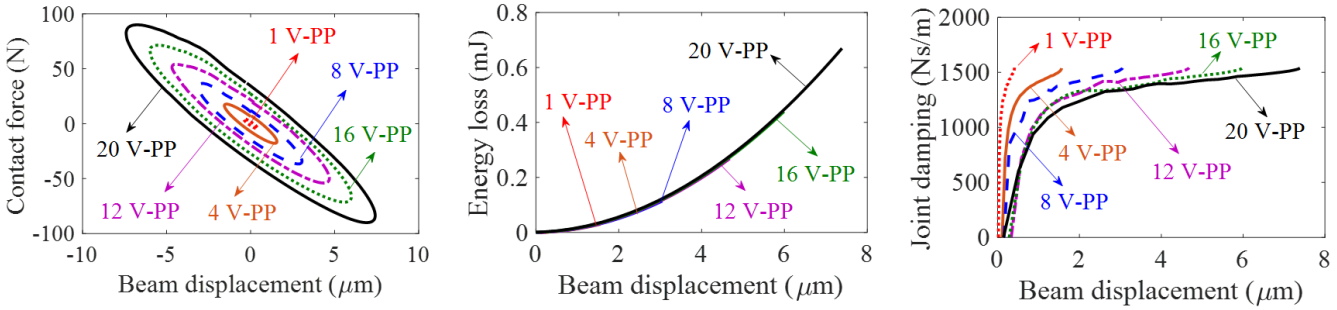

FIGURE 10. The hysteresis loops (left), the energy loss (middle), and the joint damping coefficient (right) under different excitation loads.

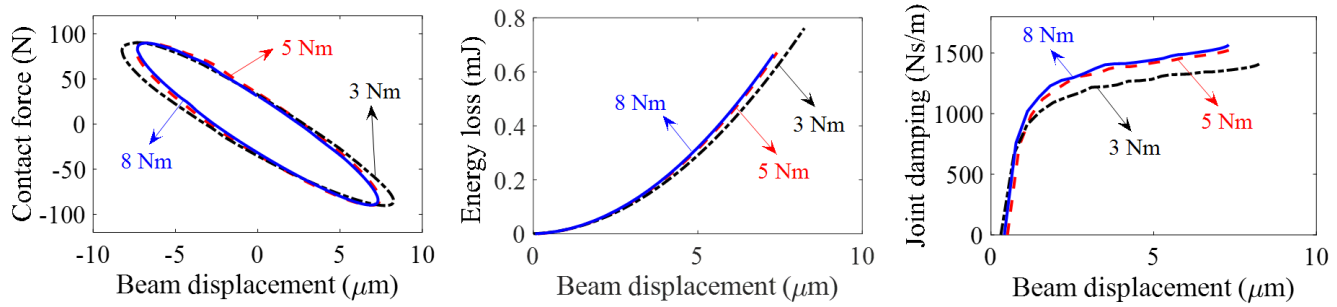

FIGURE 11. The hysteresis loops (left), the energy loss (middle), and the joint damping coefficient (right) obtained under different tightening torques.

properties, effectively. To further verify the accuracy of the proposed methods, the excitation load and the initial loading condition of the joint are changed, and the joint properties are obtained accordingly.

B. EFFECTS OF EXCITATION LOAD

The amplitude of the excitation load directly affects the hysteresis loop and the energy dissipated inside the joint. Thus, the amplitude of the harmonic load is varied from 1 V-PP to 20 V-PP. The shear forces are then measured using the nanocomposite sensor, and the relative displacements of the beams are measured through capacitive sensors. Fig. 10 shows the hysteresis loops (left), the energy loss (middle), and the joint damping coefficient (right) of the obtained at different excitation levels while the tightening torque of the bolt remains constant at 5 Nm. According to the results, the higher amplitude of the excitation load results in wider hysteresis loops and more energy loss within the joint; however, the slope of the hysteresis loop is nearly constant for all excitation loads leading to the observation that joint stiffness can be considered independent of the excitation.

Comparison of the joint damping coefficients obtained from the hysteresis loop and the joint identification algorithm shows that the deviation between the predictions of both methods remains between 10 to 17 percent for different excitation loads. Table 3 presents the joint properties obtained using the proposed methods under different excitation loads. The joint damping coefficient predicted by the hysteresis loops increases by about 8 percent when the excitation load increase from 1 V-PP to 20 V-PP. On the other hand, the joint identification algorithm results in almost the same joint damping coefficients at different excitation loads. A similar conclusion was presented by Bograd *et al.* [19] where they did not observe a significant change in the joint stiffness and damping under different excitation loads.

TABLE 3. The joint properties identified under different excitation loads.

Excitation (V-PP)	Joint property	Method		
		Joint Identification algorithm	Hysteresis loop	Diff. (%)
1.0	Energy loss (mJ)	2.052×10^{-3}	2.289×10^{-3}	10.4
	Damping (Ns/m)	1543	1727	10.7
4.0	Energy loss (mJ)	2.979×10^{-2}	3.518×10^{-2}	15.3
	Damping (Ns/m)	1538	1827	15.8
8.0	Energy loss (mJ)	0.114	0.129	11.6
	Damping (Ns/m)	1540	1766	12.8
12.0	Energy loss (mJ)	0.268	0.298	10.1
	Damping (Ns/m)	1541	1726	10.7
16.0	Energy loss (mJ)	0.439	0.517	15.1
	Damping (Ns/m)	1543	1826	15.5
20.0	Energy loss (mJ)	0.672	0.809	17.1
	Damping (Ns/m)	1542	1867	17.4

C. EFFECTS OF TIGHTENING TORQUE

The initial condition of the bolted joint may also affect the joint properties. Thus, the tightening torque of the bolt is changed between 3 Nm to 8 Nm while the system is

TABLE 4. The joint properties identified under different tightening torques.

Tightening torque (Nm)	Joint property	Method		
		Joint Identification algorithm	Hysteresis loop	Diff. (%)
3.0	Energy loss (mJ)	0.762	0.871	12.5
	Damping (Ns/m)	1410	1624	13.1
5.0	Energy loss (mJ)	0.672	0.809	17.1
	Damping (Ns/m)	1542	1867	17.4
8.0	Energy loss (mJ)	0.665	0.728	8.7
	Damping (Ns/m)	1569	1729	9.3

excited with the frequency of 400 Hz and the amplitude of 20 V-PP. Fig. 11 shows the hysteresis loops (left), the energy loss (middle), and the joint damping coefficient (right) obtained under different tightening torques. According to the results, the joint stiffness decreases by about 8 percent, from 11.8 MN/m to 10.8 MN/m, when the bolt torque is reduced from 5 Nm to 3 Nm. However, the slope of the hysteresis loop, and subsequently the stiffness of the shear layer, shows little change at different tightening torques. Using the new stiffnesses obtained for each initial condition, the stiffness of the shear layer is derived, and the energy loss and damping coefficient are found using the joint identification algorithm. Increasing the torque from 3 Nm to 8 Nm does not result in considerable changes on the energy loss and the damping coefficient. On the other hand, the damping coefficient predicted by the hysteresis loop method and the joint identification algorithm decreases by about 10 percent at a torque of 3 Nm. Table 4 summarizes the joint properties obtained from both methods under different tightening torques where the deviation remains less than 17 percent for all the loading conditions. Comparison of the obtained results from the hysteresis loops and the joint identification algorithm shows that the damping coefficient decreases when the tightening torque is either increased or decreased within a certain limit; however, the reduction of the damping coefficient is more significant at the lower tightening torques.

D. ASSUMPTIONS AND LIMITATIONS

The proposed identification method has been tested only for lap joints subjected to translational excitation and the application of the proposed methodology to other types of joints and rotational degrees of freedom requires further investigations, which is the topic of future studies. Furthermore, a circular area was considered for the sticking and sliding zones while the joint is excited harmonically from both sides. In addition, the clamping pressure was assumed to be evenly distributed under the bolt head, and the stress distribution inside the joint follows a nonlinear analytical equation, which has been derived empirically. Thus, it is expected that application of a complex joint model with nonlinear pressure distribution would result in a more accurate estimation of the joint dynamic properties. The stiffness of the elastic shear layer was also assumed to be constant throughout the identification process under certain level of excitation and loading condition.

Another important factor that may alter the contact zone and the joint properties is the fretting wear. Fretting wear results in an increase in the contact stiffness particularly during the initial loading cycles. When the joint is subject to intensive excitation loads and the transition to sliding mode occurs, the quality of the nanocomposite sensor and the contact surfaces may degrade. Therefore, a new ceramic-type nanocomposite sensor would benefit the accuracy of the proposed identification algorithm. Furthermore, it was assumed that the damping in the structure is caused by the friction force inside the joint. The other sources of damping, such as the connection between the washers, links and beams were considered negligible.

V. CONCLUSION

A new approach using polymer-based nanocomposite sensors was introduced in this study to identify dynamic properties of the bolted lap joints. The nanocomposite sensor was implemented within the joint interface to measure the contact forces while the joint is excited dynamically. The relative displacement of the bolted beams, along with the contact shear forces, were used to extract the hysteresis loop of the joint. The hysteresis loop was then used to identify the joint stiffness and damping coefficient. The joint identification algorithm based on the stick-slip transition in the contact interface was introduced to obtain the energy loss and damping coefficient of the joint. The developed techniques include part of the nonlinearities of the joint, which is usually disregarded for simplicity. The maximum deviation between the methods was about 17 percent, which is mostly due to the assumptions made regarding the stick-slip boundary identification and analytical function used to model the contact stress. It was concluded that the joint properties do not change significantly while the excitation load was varied from 1 V to 20 V peak to peak and the torque from 3 Nm to 8 Nm.

REFERENCES

[1] D. J. Segalman, "Modelling joint friction in structural dynamics," *Struct. Control Health Monit., Off. J. Int. Assoc. Struct. Control Monit. Eur. Assoc. Control Struct.*, vol. 13, no. 1, pp. 430–453, 2006.

[2] W. D. Iwan, "A distributed-element model for hysteresis and its steady-state dynamic response," *J. Appl. Mech.*, vol. 33, no. 4, pp. 893–900, Dec. 1966.

[3] C.-H. Menq, J. Bielak, and J. H. Griffin, "The influence of microslip on vibratory response, Part I: A new microslip model," *J. Sound Vib.*, vol. 107, no. 2, pp. 279–293, Jun. 1986.

[4] Y. Song, C. J. Hartwigsen, D. M. Mcfarland, A. F. Vakakis, and L. A. Bergman, "Simulation of dynamics of beam structures with bolted joints using adjusted Iwan beam elements," *J. Sound Vib.*, vol. 273, no. 1, pp. 249–276, 2004.

[5] A. T. Mathis, N. N. Balaji, R. J. Kuether, A. R. Brink, M. R. Brake, and D. D. Quinn, "A review of damping models for structures with mechanical joints," *Appl. Mech. Rev.*, vol. 72, no. 4, 2020, Art. no. 040802.

[6] M. R. W. Brake, "A reduced Iwan model that includes pinning for bolted joint mechanics," *Nonlinear Dyn.*, vol. 87, no. 2, pp. 1335–1349, Jan. 2017.

[7] N. N. Balaji, W. Chen, and M. R. W. Brake, "Traction-based multi-scale nonlinear dynamic modeling of bolted joints: Formulation, application, and trends in micro-scale interface evolution," *Mech. Syst. Signal Process.*, vol. 139, May 2020, Art. no. 106615.

[8] R. J. Kuether and D. A. Najera-Flores, "Response predictions of reduced models with whole joints," Sandia Nat. Laboratories, Albuquerque, NM, USA, Tech. Rep. SAND2018-6002C, 2018.
[9] S. Bograd, P. Reuss, A. Schmidt, L. Gaul, and M. Mayer, "Modeling the dynamics of mechanical joints," *Mech. Syst. Signal Process.*, vol. 25, no. 8, pp. 2801–2826, Nov. 2011.
[10] M. Iranzad and H. Ahmadian, "Identification of nonlinear bolted lap joint models," *Comput. Struct.*, vol.s. 96–97, pp. 1–8, Apr. 2012.
[11] A. R. Brink, R. J. Kuether, M. D. Fronk, B. L. Witt, and B. L. Nation, "Contact stress and linearized modal predictions of as-built preloaded assembly," *J. Vib. Acoust.*, vol. 142, no. 5, Oct. 2020, Art. no. 051106.
[12] R. A. Ibrahim and C. L. Pettit, "Uncertainties and dynamic problems of bolted joints and other fasteners," *J. Sound Vib.*, vol. 279, nos. 3–5, pp. 857–936, Jan. 2005.
[13] M. Sanati, Y. Terashima, E. Shamoto, and S. S. Park, "Development of a new method for joint damping identification in a bolted lap joint," *J. Mech. Sci. Technol.*, vol. 32, no. 5, pp. 1975–1983, May 2018.
[14] M. Mehrpouya, M. Sanati, and S. S. Park, "Identification of joint dynamics in 3D structures through the inverse receptance coupling method," *Int. J. Mech. Sci.*, vol. 105, pp. 135–145, Jan. 2016.
[15] M. Sanati, Y. Alammari, J. H. Ko, and S. S. Park, "Identification of joint dynamics in lap joints," *Arch. Appl. Mech.*, vol. 87, no. 1, pp. 99–113, Jan. 2017.
[16] M. Zhang, L. Lu, W. Wang, and D. Zeng, "The roles of thread wear on self-loosening behavior of bolted joints under transverse cyclic loading," *Wear*, vols. 394–395, pp. 30–39, Jan. 2018.
[17] D. J. Segalman, D. L. Gregory, M. J. Starr, B. R. Resor, M. D. Jew, J. P. Lauffer, and N. M. Ames, "Handbook on dynamics of jointed structures," Sandia Nat. Laboratories, Albuquerque, NM, USA, Tech. Rep. SAND2009-4164, 2009.
[18] E. Shamoto, Y. Hashimoto, M. Shinagawa, and B. Sencer, "Analytical prediction of contact stiffness and friction damping in bolted connection," *CIRP Ann.*, vol. 63, no. 1, pp. 353–356, 2014.
[19] S. Bograd, A. Schmidt, and L. Gaul, "Joint damping prediction by thin-layer elements," in *Proc. XXVI: Conf. Expo. Struct. Dyn. (IMAC)*, Orlando, FL, USA, Feb. 2008, pp. 1–10.
[20] B. K. Nanda and A. K. Behera, "Study on damping in layered and jointed structures with uniform pressure distribution at the interfaces," *J. Sound Vib.*, vol. 226, no. 4, pp. 607–624, 1999.
[21] C.-H. Menq, "Modeling and vibration analysis of friction joints," *J. Vib. Acoust.*, vol. 111, no. 1, pp. 71–76, Jan. 1989.
[22] E. Cigeroglu, W. Lu, and C.-H. Menq, "One-dimensional dynamic microslip friction model," *J. Sound Vib.*, vol. 292, nos. 3–5, pp. 881–898, May 2006.
[23] M. Sanati, A. Sandwell, H. Mostaghimi, and S. Park, "Development of nanocomposite-based strain sensor with piezoelectric and piezoresistive properties," *Sensors*, vol. 18, no. 11, p. 3789, Nov. 2018.

MEHDI SANATI received the Ph.D. degree in mechanical and manufacturing engineering from the University of Calgary, Canada, in 2019.

He has several years of academic and industrial work experience in the fields of dynamics, vibrations, systems design, and manufacturing technologies. He has authored more than ten articles and his research interests include vibrations and modal analysis of systems, joint dynamics identification, chatter suppression, finite element analysis of structures and machines, and nanocomposite sensor development.

HAMID MOSTAGHIMI received the B.S. and M.S. degrees in mechanical-automotive engineering from the Iran University of Science and Technology (IUST), Iran, in 2011 and 2014, respectively. He is currently pursuing the Ph.D. degree in mechanical and manufacturing engineering with the University of Calgary, Canada. As a Research Assistant, he has collaborated on different industrial projects related to dynamic design, modeling, analysis, and control of systems and structures. He has authored more than ten articles. His research interests include dynamics, vibrations, pipeline engineering, powertrain systems, hybrid and electric vehicles, and control and mechatronics.

ALLEN SANDWELL received the B.S. and M.S. degrees in mechanical and manufacturing engineering from the University of Calgary, in 2013 and 2015, respectively, where he is currently pursuing the Ph.D. degree in mechanical engineering.

He is applying his skills and knowledge toward sensors and the IoT developments as the CTO of a startup company MakeSens Inc., he helped cofound along with a few of his colleagues and his supervisor. His research interests include material science and sensor design for industrial and manufacturing applications.

JIHYUN LEE received the B.S. degree in mechanical engineering from Yonsei University, Seoul, South Korea, and the M.S. and Ph.D. degrees in mechanical engineering from the University of Michigan, Ann Arbor, USA. Prior to joining the University of Calgary, she worked for two-and-a-half years as a Senior Researcher with the Department of Ultra-Precision Machines and Systems, Korea Institute of Machinery and Materials (KIMM), South Korea. She has been working as an Assistant Professor with the University of Calgary, since February 2019. She mainly fulfilled projects at KIMM were related to vibration reduction of machines using multiple TMD systems, virtual machining, robot manipulator machining on a mobile platform, and laser tracker network development. She conducts her research on smart and sustainable mechatronic systems automation at the University of Calgary.

SIMON S. PARK received the B.S. and M.S. degrees from the University of Toronto, Canada, and the Ph.D. degree in mechanical and manufacturing engineering from the University of British Columbia, Canada.

He has worked in several companies, including IBM manufacturing, where he was a Procurement Engineer for printed circuit boards and Mass Prototyping Inc., dealing with 3D printing systems. In 2004, he has formed Multifunctional Engineering, Dynamics and Automation Laboratory (MEDAL) to investigate the synergistic integration of both subtractive and additive processes that uniquely provide productivity, flexibility and accuracy to the processing of complex components. He is also a Professor with the Department of Mechanical and Manufacturing Engineering, Schulich School of Engineering, University of Calgary. He has authored more than 200 articles. His research interests include micro machining, nano engineering, CNT nanocomposites, and alternative energy applications. He is also a Professional Engineer in Alberta, and an Associate Member of the International Academy of Production Engineers (CIRP). He held a strategic Chair position at AITF Sensing and monitoring. He is also an Associate Editor of the *Journal of Manufacturing Processes* (SME and Elsevier) and *International Journal of Precision Engineering and Manufacturing Green Technology* (Springer).